Regular Article, Biochim. Biophys. Acta

# Molecular mechanisms of action of different concentrations of ethanol in water on ordered stuctures of intercellular lipids and soft keratin in the stratum corneum

Daisuke Horita,[a, d] Ichiro Hatta,[c, e] Masato Yoshimoto,[a] Yuki Kitao,[a] Hiroaki Todo,[a] and Kenji Sugibayashi*[, a, b]

[a]*Faculty of Pharmaceutical Sciences and* [b]*Life Science Research Center, Josai University, 1-1 Keyakidai, Sakado, Saitama 350-0295, Japan;* [c]*Department of Research, Nagoya Industrial Science Research Institute, 1-13 Yotsuyadori, Chikusa-ku, Nagoya 464-0819, Japan;* [d]*Research Laboratories, Ikeda Mohando Co., Ltd., 16 Jinden, Kamiichi, Nakaniikawa, Toyama 930-0394, Japan; and* [e]*Aichi Synchrotron Radiation Center, Aichi Science & Technology Foundation, 250-3 Minamiyamaguchi-cho, Seto, Aichi 489-0965, Japan*

*To whom correspondence should be addressed. e-mail: sugib@josai.ac.jp

**Abstract**

Ethanol (EtOH) is one of the bases in topically applied medicines that promotes the skin permeation of drugs. Although the effects of EtOH have been attributed to structural modifications in the stratum corneum, the underlying mechanisms, especially the influence of different concentrations of EtOH, have not been examined extensively. Structural modifications in the stratum corneum of hairless mouse due to the application of EtOH/water mixture were herein investigated at the molecular level using synchrotron X-ray diffraction. The results revealed that all EtOH concentrations examined greatly modified the short lamellar structures containing the aqueous layer in intercellular lipids and the structure of keratin fibrils in corneocytes, which can take up hydrophilic compounds. However, the long lamellar and the hydrocarbon-chain packing structures were unaffected by EtOH. Changes to the short lamellar structures were not proportional to the concentration of EtOH. However, the keratin fibril structures changed gradually with increasing EtOH concentration. The X-ray diffraction experiments enabled the effects of different EtOH concentrations on the morphology of the stratum corneum to be assessed by using a number of experimental samples to avoid variations due to individual differences. The results indicated that alterations to the short lamellar structures appeared to be related to the skin permeability of drugs with the application of EtOH/water mixture, and monotonous structural changes in the keratin fibrils with an increase in EtOH concentration may contribute to this permeation as

supplement. These results will be useful for the development of new drug formulations containing EtOH.

**Key words** ethanol; stratum corneum; intercellular lipids; corneocyte; X-ray diffraction; hairless mouse

## 1. Introduction

Ethanol (EtOH) is widely used as a skin penetration enhancer as well as a skin disinfectant and tonic. In order for drugs to be effective at their target sites, the active ingredients in topical formulations must penetrate the skin barrier, which tightly regulates the entry of external substances. This skin barrier is mainly comprised of the stratum corneum, the outermost layer of skin, which markedly restricts the penetration of drugs. EtOH has been shown to enhance the skin permeation of drugs in topical formulations markedly. Estradiol and fentanyl dermal patches are typical examples of formulations that contain EtOH in order to enhance their absorption into the skin [1–3]. The enhancements reported in the skin permeation of drugs with the application of topical formulations containing EtOH have been attributed to structural modifications in the stratum corneum. The various mechanisms underlying the penetration-enhancing effects of EtOH on the stratum corneum barrier include lipid extraction, increase in lipid fluidity, enhancement of drug solubility in the lipids of the stratum corneum, change in skin hydration, an altered putative pore pathway, alteration in keratinized proteins, and its effects on solvent drugs [4,5]. However, the effects of EtOH on the structures of soft keratin and intercellular lipids in the stratum corneum have not been extensively examined at the molecular level.

In the present study, we thus utilized synchrotron X-ray diffraction to examine the structure of the stratum corneum at the molecular level as well as the effects of EtOH/water

mixture on the structures of intercellular lipids and fibrils in the soft keratin. We previously demonstrated that EtOH/water mixture affected the *in vitro* permeability of drugs through pig skin in an EtOH concentration-dependent manner [6]. The skin permeability of hydrophilic drugs was increased but conversely decreased by low and high concentrations of EtOH, respectively, suggesting that the effects of EtOH/water mixture on the structure of the stratum corneum may depend on its volume ratio. In the present study, we measured X-ray diffraction in the stratum corneum of mouse skin as a function of EtOH concentration. Previous studies have already used X-ray diffraction in hairless mouse skin [7,8], hairless rat skin [9], and pig skin [10,11]. Although there are slight differences in the constituents of intercellular lipids among mammalian species, the lamellae have almost the same periodical structure among the mammals. As for the skin permeation of chemical compounds, the skin of rodents, such as rat and mouse, has higher permeability than pig or human skin, whereas the structures of the stratum corneum are similar among these species. Among these mammals, the X-ray diffraction profiles of the stratum corneum in hairless mice showed the most distinct diffraction peaks, and represented the typical characteristics of the stratum corneum in mammals. Therefore, we employed hairless mouse skin in the present study to detect minute changes in the structure of the stratum corneum upon treatment with EtOH/water mixture. The diffraction profile of the stratum corneum has also been investigated in humans [12,13], and has been found to have similar characteristics to that in hairless mice.

In this study, we investigated the molecular mechanisms of action of various volume ratios in EtOH/water mixture on intercellular lipids and soft keratin based on a structural analysis using synchrotron X-ray diffraction experiments in stratum corneum treated with the mixture.

## 2. Materials and methods

### 2.1. Materials

EtOH (99.5%, HPLC grade), sodium chloride, disodium hydrogen phosphate, and potassium dihydrogen phosphate were obtained from Wako Pure Chemical Ind., Ltd. (Osaka, Japan). Trypsin and trypsin inhibitor were obtained from Sigma-Aldrich Co., Ltd. (St. Louis, MO, U.S.A.). All other reagents and solvents were of reagent grade or HPLC grade, and used without further purification.

### 2.2 Animals

Male hairless mice (HR-1, 8–9 weeks old) were obtained from Saitama Experimental Animals Supply Co., Ltd. (Sugito, Saitama, Japan). All animal studies were conducted according to the recommendations of the Institutional Board for Animal Studies, Josai University (Sakado, Saitama, Japan).

### 2.3. Sample preparation process

Hairless mouse skin was separated from the abdominal and dorsal region. After the

removal of excess fat, the skin was soaked with 0.1% (w/v) trypsin in pH 7.4 phosphate-buffered saline (PBS) at 4˚C for 16 h. After being incubated for another 4 h at 37˚C, the stratum corneum was separated from the skin. It was then treated with 0.1% (w/v) trypsin inhibitor and rinsed in distilled water three times. Following this, EtOH/water mixture of 0/100, 20/80, 40/60, 60/40, 80/20 or 100/0 v/v% was applied to the dried stratum corneum for 2 h. By reducing the content of EtOH/water mixture from stratum corneum treated by the mixture the EtOH/water mixture content in the stratum corneum was adjusted to be 20 wt%. An approximately 5-mg piece of the sample was placed into a capillary glass tube and immediately sealed for the X-ray diffraction experiment. We used 25 mice in the experiment and obtained four samples per mouse. In addition, 13–14 samples were used for each experiment; the samples treated by EtOH/water mixture were randomly selected in order to avoid excessive use of a specific region or specific individual.

2.4. X-ray diffraction study

The X-ray diffraction study was performed at the beamline BL40B2 (Structural Biology II Beamline) of SPring-8 (Harima, Hyogo, Japan). X-ray diffraction profiles were recorded using an imaging plate system (R-AXIS IV; Rigaku Corporation, Tokyo, Japan) with a 30 cm × 30 cm area. The X-ray wavelength was 0.0709 nm and sample-to-detector distance was approximately 500 mm. Reciprocal spacing [$S = (2 / \lambda) \times \sin \theta$] was calibrated from the lattice spacing ($d$ = 5.838 nm, where $d$ is the lamellar repeat distance) of silver

behenate at room temperature, where $2\theta$ is the scattering angle. The exposure time was 15 s. The diffraction pattern was circularly averaged in order to obtain the radial intensity profile. The profile was obtained from samples with almost the same weight of stratum corneum. Photon counting for the profile was performed at 1152 pixels in the range of $S$ = 0.05–3.0 $nm^{-1}$, and we counted the photon number at each pixel.

## 3. Results

### 3.1. Effects of various volume ratios in EtOH/water mixture on the ordered structure of intercellular lipids

Figure 1 shows the X-ray diffraction profiles ($S$ = 0.05–3.0 $nm^{-1}$) of the stratum corneum of hairless mice following treatments with various volume ratios in EtOH/water mixture. We determined the X-ray diffraction pattern from approximately one dozen stratum corneum samples with almost the same volume after the application of EtOH/water mixture at each volume ratio. Diffraction peaks were due to the repeat distances of the lamellar structures in the small-angle region as well as the lattice constants of the lateral hydrocarbon-chain packing structures in the wide-angle region. Figure 2a shows the X-ray diffraction profiles in the small-angle region within the range of $S$ = 0.10–0.40 $nm^{-1}$. Three partially overlapping peaks derived from the short and long lamellar structures were detected within the range of $S$ = 0.12–0.25 $nm^{-1}$, and these profiles changed according to the volume

ratio. In addition, the single diffraction peaks derived from the long and short lamellar structures were observed near $S$ = 0.30 and $S$ = 0.37, respectively. Figure 2b shows the X-ray diffraction profiles in the wide-angle region within the range of $S$ = 2.0–3.0 $nm^{-1}$. Two diffraction peaks near $S$ = 2.4 $nm^{-1}$ and $S$ = 2.7 $nm^{-1}$ corresponded to the hexagonal and orthorhombic hydrocarbon-chain packing structures and only the orthorhombic hydrocarbon-chain packing structures, respectively. In this experiment, the stratum corneum sample from hairless mice showed split peaks for the orthorhombic hydrocarbon-chain packing structures near $S$ = 2.7 $nm^{-1}$.

**Figs. 1 and 2**

3.2. Analysis of multiple diffraction peaks in the small-angle region

Multiple partially overlapping peaks in the small-angle region in the range of $S$ = 0.12–0.25 $nm^{-1}$ in Figure 2a were analyzed by fitting to Gaussian curves. Figures 3a and 3b show the results obtained by the Gaussian curve fitting analysis for the small-angle X-ray diffraction profiles of the stratum corneum in hairless mice after treatments with EtOH/water mixture of 60/40 and 100/0 v/v%, respectively. The 2nd order diffraction of the long lamellar structure, the 1st order diffraction of the short lamellar structure, and the 3rd order diffraction of the long lamellar structure occurred in the region from $S$ = 0.12 to 0.25 $nm^{-1}$ [12,14]. In

order to present typical examples of the fitting analysis, Figures 3a and 3b show those for EtOH/water mixture of 60/40 and 100/0 v/v%, respectively, where the diffraction profiles fit well to the sum of three Gaussian curves and a linear background. Figure 3c shows the results obtained by the Gaussian curve fitting analysis for 4th order diffraction peak of the long lamellar structures at EtOH/water mixture of 100/0 v/v%. Although the 2nd and 3rd order diffraction peaks of the long lamellar structures overlap with other peaks, the 4th order diffraction peak was obtained as a single peak with a flat background and has adequate strength for fitting analysis. Therefore, the 4th diffraction peak was used for the analysis to show the change of the long lamellar structures more precisely. Table 1 shows the repeat distances of the long and short lamellar structures and the full widths at half maximum of the diffraction peaks as a function of the volume ratios in EtOH/water mixture. In order to compare variations in the short and long lamellar structures, the normalized repeat distance and normalized full width at half maximum are shown in Figure 4.

The application of EtOH/water mixture did not significantly affect the long lamellar spacing and the peak width. On the other hand, the short lamellar spacing was minimal and the peak width was maximal after treatment with EtOH/water mixture of 60/40 v/v%. Thus, EtOH/water mixture was involved in both regularly and irregularly alteration on the periodic pattern of the short lamellar structure in an EtOH concentration-dependent manner.

**Fig. 3, Table 1, and Fig. 4**

3.3 Analysis of diffraction peaks in the wide-angle region

As shown in Figure 2b, two diffraction peaks (near $S$ = 2.4 $nm^{-1}$ and near $S$ = 2.7 $nm^{-1}$) derived from the hexagonal and orthorhombic hydrocarbon-chain packing structures were detected in the wide-angle region. The peak near $S$ = 2.7 $nm^{-1}$ was actually composed of two peaks. We analyzed these peaks by fitting to two Gaussian curves, similar to that shown in Figure 3. The split peak was consequently separated into two peaks ($S$ = 2.64 $nm^{-1}$ and $S$ = 2.67 $nm^{-1}$), and the total diffraction profile fit well to the sum of the two Gaussian curves. We then calculated the lattice spacing and the peak widths from those diffraction peaks. Figures 5 and 6 show the effects of the treatments with EtOH/water mixture on the lattice spacing and the normalized full widths at half maximum, respectively. The lattice spacing and peak widths for the hexagonal and orthorhombic hydrocarbon-chain packing structures were almost constant and independent of the EtOH concentration.

**Figs. 5 and 6**

3.4. Effects of various volume ratios in EtOH/water mixture on the soft keratin in corneocytes

We analyzed a broad diffraction peak at approximately $S$ = 1.0 $nm^{-1}$. This broad peak

has previously been shown to be derived from the soft keratin, which is loosely packed in corneocytes [10]. Figure 7 shows X-ray diffraction profiles in the region within $S$ = 0.5–1.5 $nm^{-1}$ in the stratum corneum of hairless mice treated with various volume ratios in EtOH/water mixture. To calculate the peak position and the width, Gaussian curve fitting analysis was again applied to each diffraction profile. Figure 8 shows the effects of various volume ratios in EtOH/water mixture on the reciprocal of the peak position (protofibril distance) and the full width at half maximum obtained from the diffraction profile for the soft keratin. The protofibril distance and the peak width increased in an EtOH concentration-dependent manner. Therefore, EtOH perturbed the soft keratin structure, which loosened fibril packing.

**Figs. 7 and 8**

## 4. Discussion

In the present study, we performed X-ray diffraction experiments on the stratum corneum of hairless mice to investigate the effects of EtOH/water mixture on its structure. We applied different volume ratios in EtOH/water mixture to the stratum corneum, and then examined its structure using X-ray diffraction in the SPring-8 facility. The EtOH/water mixture content in stratum corneum samples was prepared at 20 wt% because the water

content in the skin surface was estimated to be 20–30% [15] and mostly stabilizes the lamellar structure at this level [16]. There have been difficulties associated with comparing the results obtained from X-ray diffraction experiments on multiple samples under different conditions because the diffraction profiles of the stratum corneum are greatly affected by individual variations and/or skin sites. Few X-ray diffraction studies have closely examined the effects of EtOH/water mixture on the structure of the stratum corneum. In this study, we prepared approximately one dozen skin samples per concentration of EtOH and the X-ray diffraction patterns obtained; therefore, differences due to individual variations and/or skin sites were avoided and the influence of skin treatments with any volume ratio in EtOH/water mixture on the structure of the stratum corneum could be compared clearly.

Ordered lamellar structures, such as the long and short lamellar structures, have periodic structures in the direction of the long axis of the hydrocarbon chain. Previous studies reported that the repeat distances of the long and short lamellar structures were approximately 13 nm and 6 nm, respectively [12,14]. To detect minute variations in the lamellar structures, the 1st order diffraction peak for the short lamellar structures, in particular, must be carefully isolated since this peak was weaker than that for the long lamellar structures. Gaussian curve fitting analysis was performed to isolate individual peaks from each other. As a result, the repeat distance and the full width at half maximum were obtained for the short lamellar structures.

Diffraction peak analyses revealed that EtOH/water mixture influenced the short lamellar structures more than the long ones. The observation of the short lamellar structure in hydrated condition was first reported experimentally by Bouwstra *et al.* [7,10,12] who have been careful for proposing the swelling behavior. They have pointed out that the X-ray diffraction peak for the short lamellar structure becomes sharp near the water content of 20 wt% but the swelling effect on the short lamellar structure was not detectable in human [12] and also hairless mouse [7] stratum corneum. On the other hand, in pig stratum corneum they have observed a weak swelling effect [10], and from a careful study on much attention to the effect of water in hairless mouse stratum corneum Ohta *et al.* have found the swelling behavior with increasing the water content [16]. So far in various studies, the diffraction peak of short lamellar structure is sometimes undetectable [12,14], sometimes is only observed only as a shoulder [7,10] and sometimes gives rise to a clear peak [16]. In addition to these studies much clearly the swelling behavior in short lamellar structure has been observed from the neutron diffraction by Charalambopoulou *et al.* [17]. The neutron diffraction experiment by using heavy water is a powerful tool to observe the aqueous layer in stratum corneum since the layer of heavy water can be observed dominantly. It is worthwhile to point out that the increment of the spacing of short lamellar structure with increasing the water content in the previous X-ray diffraction study [16] is consistent with the neutron diffraction study [17]. Furthermore, recently Nakazawa *et al.* have proposed that based upon the X-ray diffraction

study on the swelling behavior of short lamellar structure in human stratum corneum it could involve in adjustment of the water content in stratum corneum [18]. The above fact indicates that a uniform swelling of short lamellar structure takes place in stratum corneum since X-ray and neutron diffraction measurement provide evidence for coherent structural alteration and resultantly uniform swelling of the aqueous layer. The latter fact could be rationally supposed from the swelling behavior under water obtained from the X-ray diffraction study on egg lecithin bilayers which are composed of amphiphilic molecules [19] since intercellular lipids in stratum corneum are composed of amphiphilic molecules such as ceramides and fatty acids. Therefore the aqueous layers in the short lamellar structure could take place in the face-to-face arrangement of the polar head groups via the aqueous layer. Hence, applied water or EtOH on the stratum corneum might penetrate the aqueous layer, and the behavior of the aqueous layer following the application of various volume ratios in EtOH/water mixture may depend on differences in the interactions of a water molecule and an EtOH molecule with the polar head groups of ceramides and fatty acids. The applied EtOH seems to combine with the interface between the aqueous layer and the polar head groups of ceramides and fatty acids by the hydroxyl group of an EtOH molecule facing the aqueous layer [20]. As a result, the repeat distance of the short lamellar structures decreased with an increase in the EtOH concentration in the range of EtOH/water ratio from 0/100 v/v% to 60/40 v/v%, which then conversely increased when the concentration of EtOH was elevated above 60/40 v/v%. The diffraction

peak width increased with an increase in the EtOH concentration in the range of EtOH/water ratio from 0/100 v/v% to 60/40 v/v%, but decreased with further increases in the EtOH concentration above 60/40%. These results indicate that treatment with a low concentration of EtOH disturbs the short lamellar structures, but on the other hand, treatment with a high concentration of it causes an aligned structure. In the case of treatment with mostly water or EtOH, water and EtOH molecules may exist as structured molecules in highly concentrated water and upon high EtOH, respectively. At intermediate concentrations, water and EtOH may not form structured molecules, so the layer structure may be disrupted. In addition, Kwak *et al.* reported [21] the effect of various concentrations of EtOH on model membranes of stratum corneum lipids composed of different lipid classes. They pointed out that lipid model membranes including ceramides were disrupted by the action of EtOH compared with those with free fatty acids. This might indicate that there is less ceramide in the short lamellar structures, being susceptible to EtOH, than in the long lamellar structures.

On the other hand, the hexagonal and orthorhombic hydrocarbon-chain packing structures observed on a plane perpendicular to the long axis of the hydrocarbon chain were previously reported to have lattice constants of 0.42 nm, 0.42 nm, and 0.37 nm [22]. Since the diffraction profile with split peaks near $S = 2.7$ nm$^{-1}$ fits well to the sum of the two Gaussian curves and a background line, there may be at least two types of orthorhombic hydrocarbon-chain packing structure in the intercellular lipids in the stratum corneum of the

hairless mice used in the present study. The lattice constants and the peak widths derived from the hexagonal and the orthorhombic hydrocarbon-chain packing structures were not influenced by the treatment with any volume ratio in EtOH/water mixture.

Corneocytes, which are surrounded by intercellular lipids, are crucially involved in maintaining the form of skin tissue. Cross-sectional observations of the stratum corneum using electron microscopy indicated that it is composed of a higher proportion of corneocytes than intercellular lipids [23]. The interior of corneocytes is filled with agglutinated-keratin fibers. A diffraction peak of loosely packed soft keratin fibers was previously detected near $S$ = 0.96 $nm^{-1}$ in the middle-angle region [10]. Thus, the reciprocal of the peak position corresponded to the protofibril-to-protofibril distance. This diffraction peak was also observed and analyzed in the present study. The protofibril distance and peak width increased in an EtOH concentration-dependent manner. This result indicates that EtOH penetrated the corneocytes [24] and disturbed the soft keratin structure by loosening fibril packing in the corneocytes in an EtOH concentration-dependent manner. This phenomenon may be involved in the denaturation effects of EtOH on keratin proteins.

The results of the present study reveal the molecular mechanisms of action of different volume ratios in EtOH/water mixture on the ordered structures of intercellular lipids and soft keratin in the stratum corneum. All volume ratios in EtOH/water mixture greatly affected the short lamellar structure in the intercellular lipids and the fibril structures of the

soft keratin, but had a negligible effect on the long lamellar structures in the intercellular lipids and the hydrocarbon-chain packing structures. The structural alteration in the stratum corneum due to the application of EtOH/water mixture suggests that it is heavily involved in the skin permeability of topically applied drugs in formulations containing both EtOH and water. We previously reported the effects of EtOH/water mixture on the skin permeability of drugs using an *in vitro* pig skin permeation test [6], and demonstrated that the skin permeability of hydrophilic drugs was increased by a low concentration of EtOH and, on the other hand, was decreased by a high concentration of it. Although changes in the diffusivity and partition coefficient of penetrants were expected with the EtOH/water mixture treatment, the molecular mechanisms underlying the skin permeability of drugs have not yet been fully elucidated. In the present study, the periodic structures in short lamellar became irregular at low to medium concentrations of EtOH, but return to regular at higher concentrations of EtOH. However in the orthogonal direction to the periodic structure the hydrocarbon-chain packing structure does not change. Therefore not only water but also EtOH does not affect the hydrocarbon-chain packing and EtOH/water mixture causes disarrangement of the regular short lamellar structure with the aqueous layers. The structure of the soft keratin was altered gradually by increases in the EtOH concentration. Therefore, these changes may be strongly associated with the skin permeability of chemical compounds. The skin penetration of chemical compounds through the stratum corneum depends on drug partition to the stratum

corneum and drug diffusivity in drug-distributed regions. Lipophilic compounds have been considered to be distributed to the hydrophobic region in intercellular lipids and then diffuse in the lipid pathway, and as a result, the compounds penetrate the skin. In contrast, hydrophilic compounds are considered to be distributed to the aqueous regions in intercellular lipids or corneocytes and diffusion is observed in the aqueous pathway. Accordingly, the changes to the short lamellar and soft keratin structures due to the application of EtOH/water mixture imply that the distribution to aqueous regions and the diffusivity of hydrophilic compounds may be altered. Since EtOH/water mixture did not significantly influence the long lamellar structures with hydrophobic characteristics, the distribution and the diffusivity of lipophilic compounds may be slightly changed compared with those of hydrophilic compounds. Thus, EtOH treatment can greatly affect the skin permeation of hydrophilic compounds. Although hairless mouse skin was selected for the collection of stratum corneum samples in the present study, the influence of EtOH/water mixture was previously shown to be similar on the skin of other animals (pig and rat) including human. The above results are consistent with the previous findings of an *in vitro* skin permeation study using pig skin [6]. Further studies are needed to clarify the relationship between the structure of the stratum corneum and skin permeability of chemical compounds following EtOH/water mixture treatment. In particular, research that reveals the relative amounts of short lamellar structures and long lamellar structures appears to be important, since determination of their ratio has not

been accomplished yet. For the quantitative consideration we need statistical analysis of the present data. For this purpose additionally there is room for further research into statistical analysis.

EtOH is an ingredient in vehicles for topically applied medicines. In the present study, the effect of EtOH/water mixture on the structure of the stratum corneum was not directly proportional to its volume ratio. Although EtOH/water mixture changed the structure of the stratum corneum, the type of change was largely dependent on its volume ratio. Various concentrations of EtOH are currently selected for topically applied medicines. Therefore, the effects of EtOH concentrations on the structure of the stratum corneum as well as drug efficacy and safety must be considered when developing preparations containing both EtOH and water.

**Acknowledgment**

We would like to thank Dr. Noboru Ohta for help during the data collection at BL40B2 in the SPring-8 facility. The experiment was conducted under the approval of the SPring-8 Proposal Review Committee (proposal number 2012B1255).

**References**

[1] L. K. Pershing, L. D Lambert., K. Knutson, Mechanism of ethanol-enhanced estradiol

permeation across human skin *in vivo*, Pharm. Res. 7 (1990) 170–175.

[2] W. R. Good, M. S. Powers, P. Campbell, L. Schenkel, A new transdermal delivery system for estradiol, J. Control. Release 2 (1985) 89–97.

[3] B. Berner., G. C. Mazzenga, J. H. Otte, R. J. Steffens, R. H. Juang, C. D. Ebert, Ethanol: water mutually enhanced transdermal therapeutic system II: skin permeation of ethanol and nitroglycerin, J. Pharm. Sci. 78 (1989) 402–407.

[4] A. C. Williams, B. W. Barry, Penetration enhancers, Adv. Drug Deliv. Rev. 56 (2004) 603–618.

[5] D. Van der Merwe, J. E. Riviere, Comparative studies on the effects of water, ethanol and water/ethanol mixtures on chemical partitioning into porcine stratum corneum and silastic membrane, Toxicol. *In vitro*. 19 (2005) 69–77.

[6] D. Horita, H. Todo, K. Sugibayashi. Effect of ethanol pretreatment on skin permeation drugs, Biol. Pharm. Bull. 35 (2012) 1343–1348.

[7] J. A. Bouwstra, G. S. Gooris, J. A. Van der Spek, S. Lavrijsen, W. Bras, The lipid and protein structure of mouse stratum corneum: a wide and small angle diffraction study, Biochim. Biophys. Acta 1212 (1994) 183–192.

[8] I. Hatta, N. Ohta, S. Ban, H. Tanaka, S. Nakata, X-ray diffraction study on ordered, disordered and reconstituted intercellular lipid lamellar structure in stratum corneum, Biophys. Chem. 89 (2001) 239–242.

[9] Y. Obata, I. Hatta, N. Ohta, N. Kunizawa, N. Yagi, K. Takayama, Combined effects of ethanol and l-menthol on hairless rat stratum corneum investigated by synchrotron X-ray diffraction, J. Control. Release 115 (2006) 275–279.

[10] J. A. Bouwstra, G. S. Gooris, W. Bras, D. T. Downing, Lipid organization in pig stratum corneum, J. Lipid Res. 36 (1995) 685–695.

[11] M. Fujii, Y. Takeda, M. Yoshida, N. Utoguchi, M. Matsumoto, Y. Watanabe, Comparison of skin permeation enhancement by 3-l-menthoxypropane-1,2-diol and *l*-menthol: the permeation of indomethacin and antipyrine through Yucatan micropig skin and changes in infrared spectra and X-ray diffraction patterns of stratum corneum, Int. J. Pharm. 258 (2003) 217–223.

[12] J. A. Bouwstra, G. S. Gooris, J. A. Van der Spek, W. Bras, Structural investigations of human stratum corneum by small-angle X-ray scattering, J. Invest. Dermatol. 97 (1991) 1005–1012.

[13] J. A. Bouwstra, G. S. Gooris, M. A. Salomons-de Vries, J. A. Van der Spek, W. Bras, Structure of human stratum corneum as a function of temperature and hydration: A wide-angle X-ray diffraction study, Int. J. Pharm. 85 (1992) 205–216.

[14] I. Hatta, N. Ohta, K. Inoue, N. Yagi, Coexistence of two domains in intercellular lipid matrix of stratum corneum, Biochim. Biophys. Acta 1758 (2006) 1830–1836.

[15] I. H. Blank, Factors which influence the water content of the stratum corneum, J. Invest.

Dermatol. 18 (1952) 443–440.

[16] N. Ohta, S. Ban, H. Tanaka, S. Nakata, I. Hatta, Swelling of intercellular lipid lamellar structure with short repeat distance in hairless mouse stratum corneum as studied by X-ray diffraction, Chem. Phys. Lipids 123 (2003) 1–8.

[17] G. Ch. Charalambopoulou, Th. A. Steriotis, Th. Hauss, A. K. Stubos, N. K. Kanellopoulos, Structural alterations of fully hydrated human stratum corneum, Physica B 350 (2004) 603–606.

[18] H. Nakazawa, N. Ohta, I. Hatta, A possible regulation mechanism of water content in human stratum corneum via intercellular lipid matrix, Chem. Phys. Lipids, 165 (2012) 238–243.

[19] Y. K. Levine, M. H. F. Wilkins, Structure of oriented lipid bilayers, Nature New Biology, 230 (1971) 69–72.

[20] T. Adachi, H. Takahashi, K. Ohki, I. Hatta, Interdigitated structure of phospholipid-alcohol systems studied by X-ray diffraction, Biophys. J. 68 (1995) 1850–1855.

[21] S. Kwak, E. Brief, D. Langlais, N. Kitson, M. Lafleur, J. Thewalt, Ethanol perturbs lipid organization in models of stratum corneum membranes: An investigation combining differential scanning calorimetry, infrared and $^{2}H$ NMR spectroscopy, Biochim. Biophys. Acta 1818 (2012) 1410–1419.

[22] G. S. Pilgram, A. M. Engelsma-van Pelt, J. A. Bouwstra, H. K. Koerten, Electron diffraction provides new information on human stratum corneum lipid organization studied in relation to depth and temperature, J. Invest. Dermatol. 113 (1999) 403–409.

[23] L. Norlén, A. Al-Amoudi, Stratum corneum keratin structure, function, and formation: the cubic rod-packing and membrane templating model, J. Invest. Dermatol. 123 (2004) 715–732.

[24] I. Hatta, H. Nakazawa, Y. Obata, N. Ohta, K. Inoue, N. Yagi, Novel method to observe subtle structural modulation of stratum corneum on applying chemical agents, Chem. Phys. Lipids 163 (2010) 381–389.

**Figure Legends**

Fig. 1. X-ray diffraction profiles in the hairless mouse stratum corneum as a function of the volume ratios in EtOH/water mixture, where *n* is the number of stratum corneum samples.

Fig. 2. Small-angle X-ray diffraction profiles (a) and wide-angle X-ray diffraction profiles (b) in the hairless mouse stratum corneum as a function of the volume ratios in EtOH/water mixture, where *n* is the number of stratum corneum samples.

Fig. 3. Typical curve fitting analysis to small-angle X-ray diffraction profiles of the stratum corneum of hairless mice treated with EtOH/water mixture of 60/40 v/v% (a) and 100/0 v/v% (b, c). The thin solid line shows the mean of raw small-angle X-ray diffraction profiles. The thick solid line indicates the best-fitted curve composed of the sum of Gaussian dotted curves and a linear background dotted line.

Fig. 4. Effects of EtOH/water mixture treatment on the repeat distances (○ or ●) and the full widths at half maximum (△ or ▲) for the 4th order diffraction of the long lamellar structures and the 1st order diffraction of the short lamellar structures. The normalized data were calculated by dividing the values of repeat distances and full width at half maximum with EtOH/water mixture treatments by those for 0/100 v/v%. The open circle or open triangle

and the closed circle or closed triangle show the long lamellar structures and the short lamellar structures, respectively.

Fig. 5. Effects of EtOH/water mixture treatment on the lattice constants for the diffraction peaks at $S$ = 2.4 $nm^{-1}$, $S$ = 2.64 $nm^{-1}$, and $S$ = 2.67 $nm^{-1}$. The open circle, open triangle, and open square show the diffraction peaks at $S$ = 2.4 $nm^{-1}$, $S$ = 2.64 $nm^{-1}$, and $S$ = 2.67 $nm^{-1}$, respectively.

Fig. 6. Effects of EtOH/water mixture treatment on the normalized full widths at half maximum for the diffraction peaks at $S$ = 2.4 $nm^{-1}$, $S$ = 2.64 $nm^{-1}$, and $S$ = 2.67 $nm^{-1}$. The normalized data were calculated by dividing the values of full width at half maximum with EtOH/water mixture treatments by those for 0/100 v/v%. The open circle, open triangle, and open square show the diffraction peak at $S$ = 2.4 $nm^{-1}$, $S$ = 2.64 $nm^{-1}$, and $S$ = 2.67 $nm^{-1}$, respectively.

Fig. 7. Medium-angle X-ray diffraction profiles in the hairless mouse stratum corneum as a function of the volume ratios in EtOH/water mixture, where $n$ is the number of stratum corneum samples.

Fig. 8. Effects of EtOH/water mixture treatment on the reciprocal of the peak position (○) and the full width at half maximum (△) for the soft keratin

# Change to the short lamellar structure in intercellular lipids

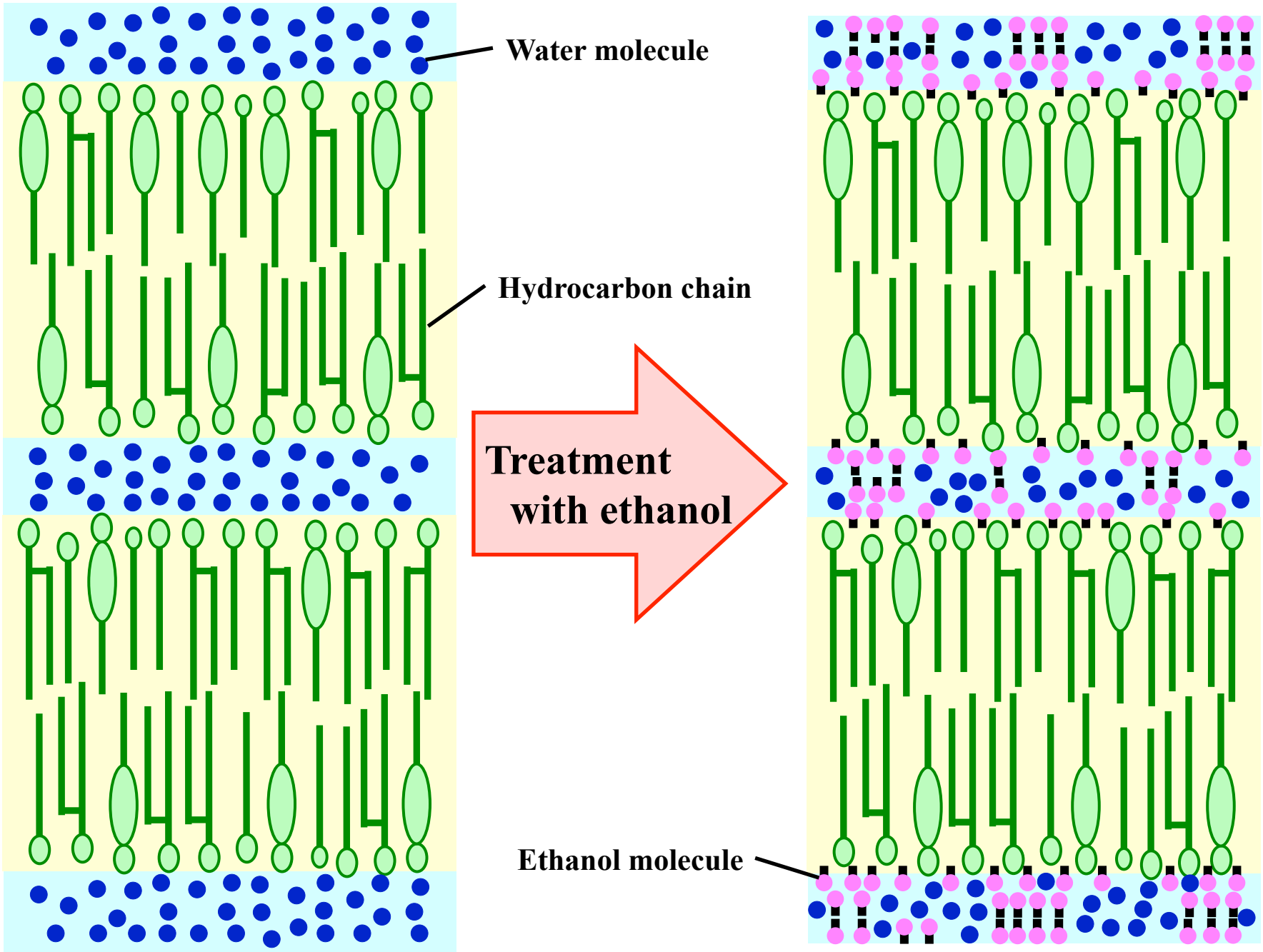

Table 1. The repeat distance (a) and full width at half maximum (b) obtained from the 4th order diffraction peak for the long lamellar structure and the 1st order diffraction peak for the short lamellar structure as a function of the volume ratios in EtOH/water mixture.

a) Repeat distance (nm)

| EtOH/water ratio (v/v %) | 0/100 | 20/80 | 40/60 | 60/40 | 80/20 | 100/0 |
|---|---|---|---|---|---|---|
| Long lamellar structure | 13.26 | 13.30 | 13.30 | 13.33 | 13.30 | 13.17 |
| Short lamellar structure | 6.29 | 6.13 | 6.13 | 5.86 | 5.95 | 6.42 |

b) Full width at half maximum ($\times 10^{-2}$ $nm^{-1}$)

| EtOH/water ratio (v/v %) | 0/100 | 20/80 | 40/60 | 60/40 | 80/20 | 100/0 |
|---|---|---|---|---|---|---|
| Long lamellar structure | 0.93 | 0.89 | 0.89 | 0.91 | 0.85 | 0.88 |
| Short lamellar structure | 1.84 | 2.59 | 2.52 | 2.83 | 1.97 | 1.33 |

Fig. 1

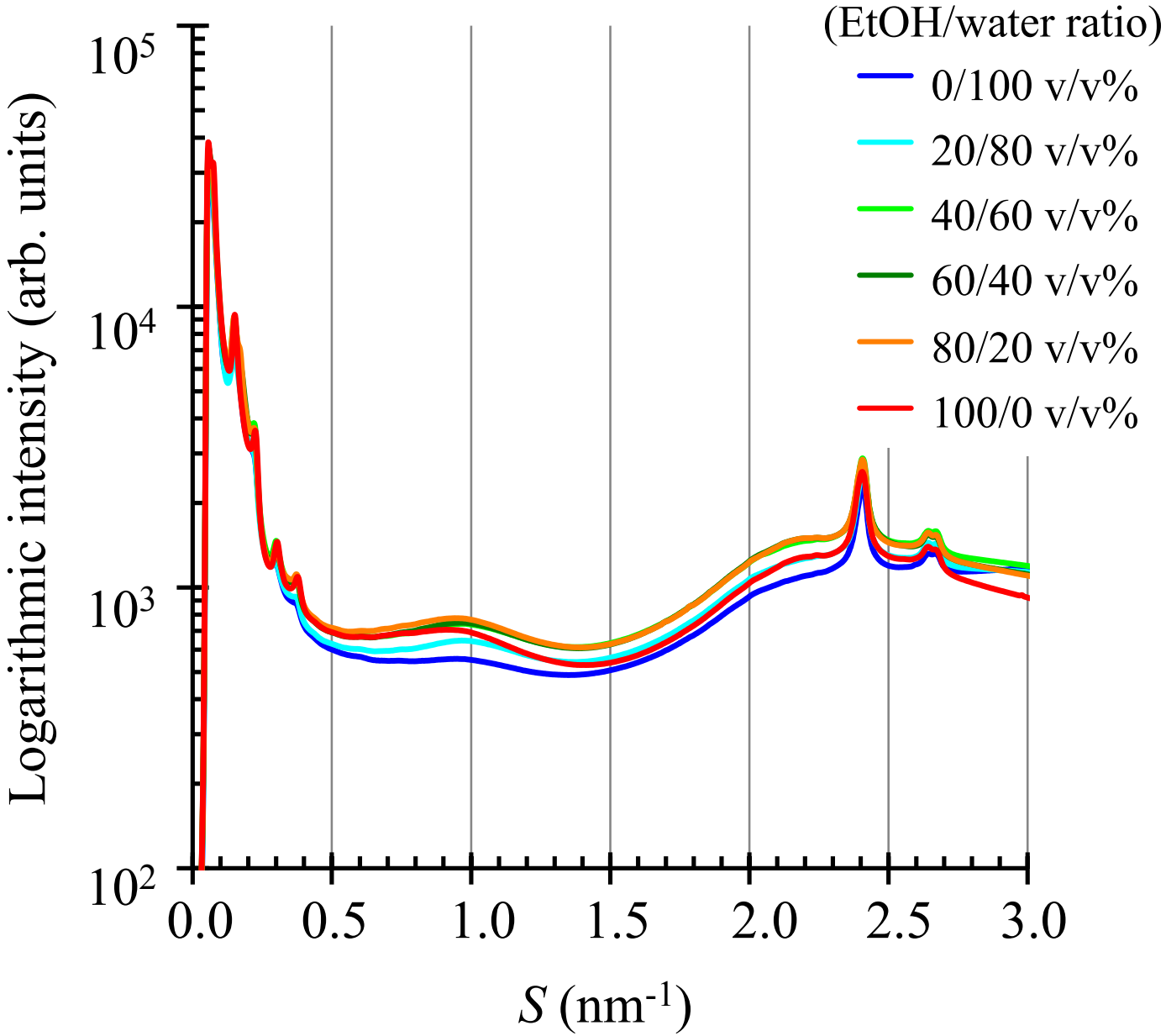
(EtOH/water ratio)
0/100 v/v%
20/80 v/v%
40/60 v/v%
60/40 v/v%
80/20 v/v%
100/0 v/v%
Logarithmic intensity (arb. units)
10^5
10^4
10^3
10^2
0.0
0.5
1.0
1.5
2.0
2.5
3.0
S (nm^-1)

**a** Fig. 2

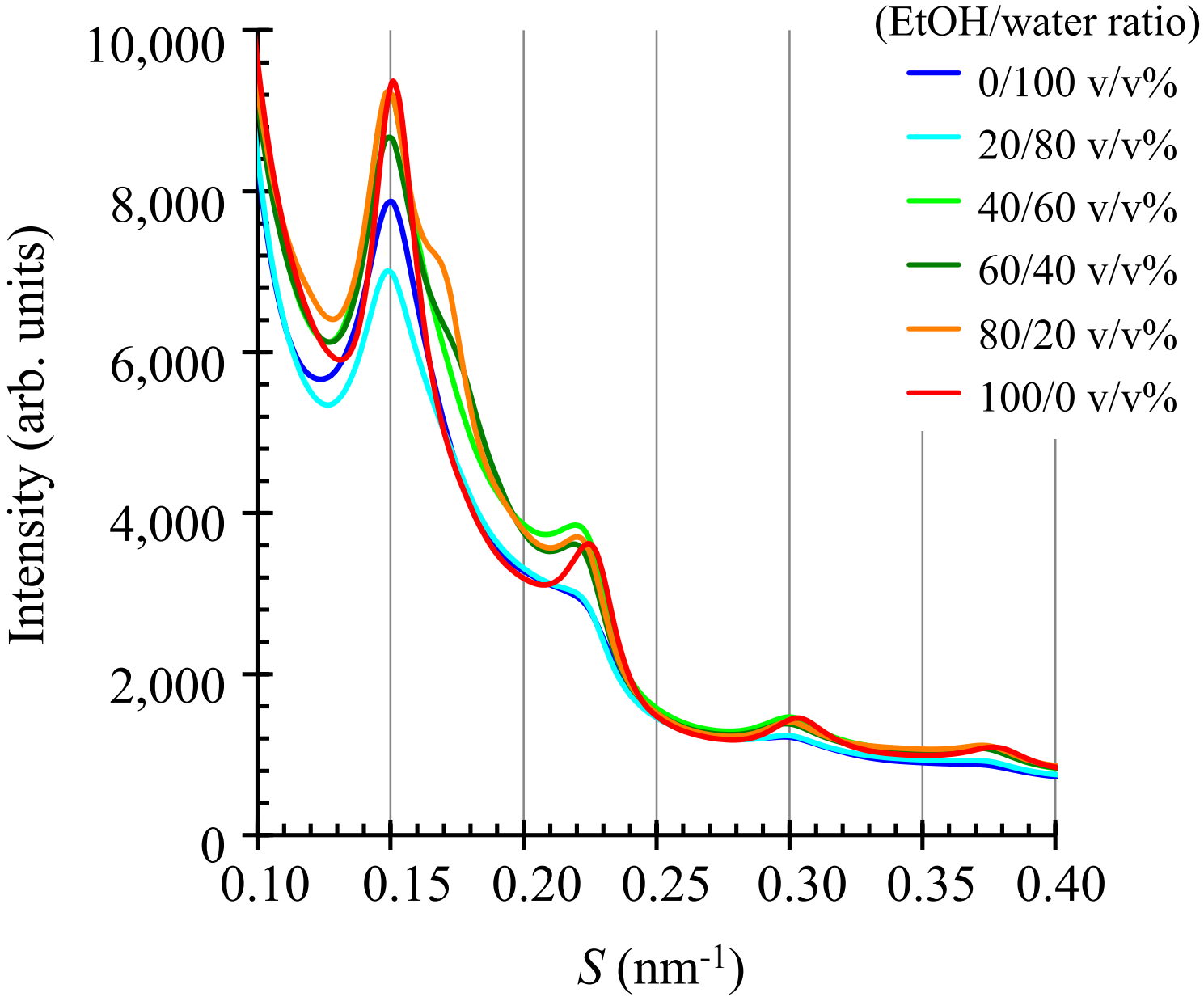
(EtOH/water ratio)
0/100 v/v%
20/80 v/v%
40/60 v/v%
60/40 v/v%
80/20 v/v%
100/0 v/v%
Intensity (arb. units)
10,000
8,000
6,000
4,000
2,000
0
0.10
0.15
0.20
0.25
0.30
0.35
0.40
S (nm-1)

**b** Fig. 2

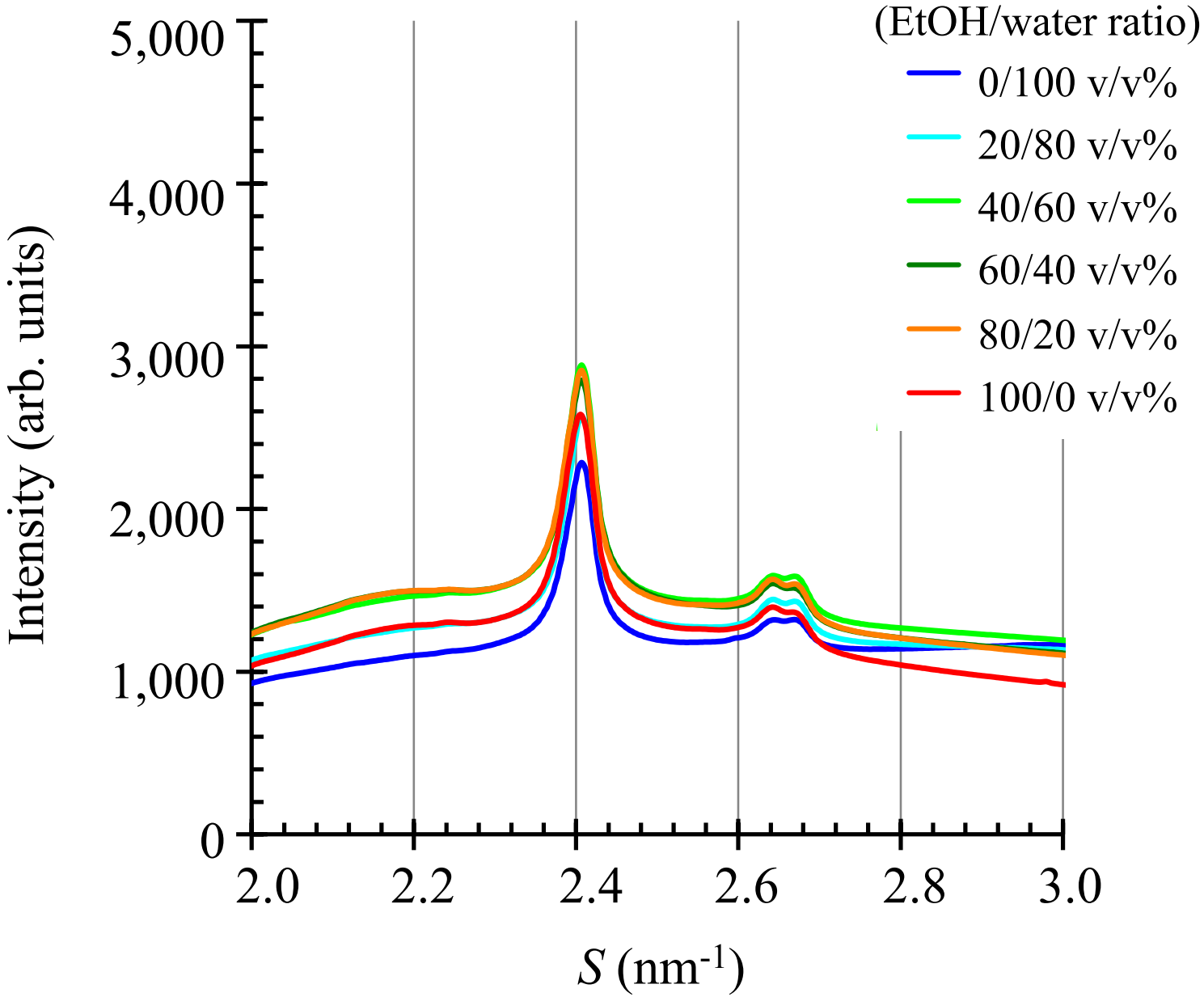
(EtOH/water ratio)
0/100 v/v%
20/80 v/v%
40/60 v/v%
60/40 v/v%
80/20 v/v%
100/0 v/v%
Intensity (arb. units)
5,000
4,000
3,000
2,000
1,000
0
2.0
2.2
2.4
2.6
2.8
3.0
S (nm-1)

**a** Fig. 3

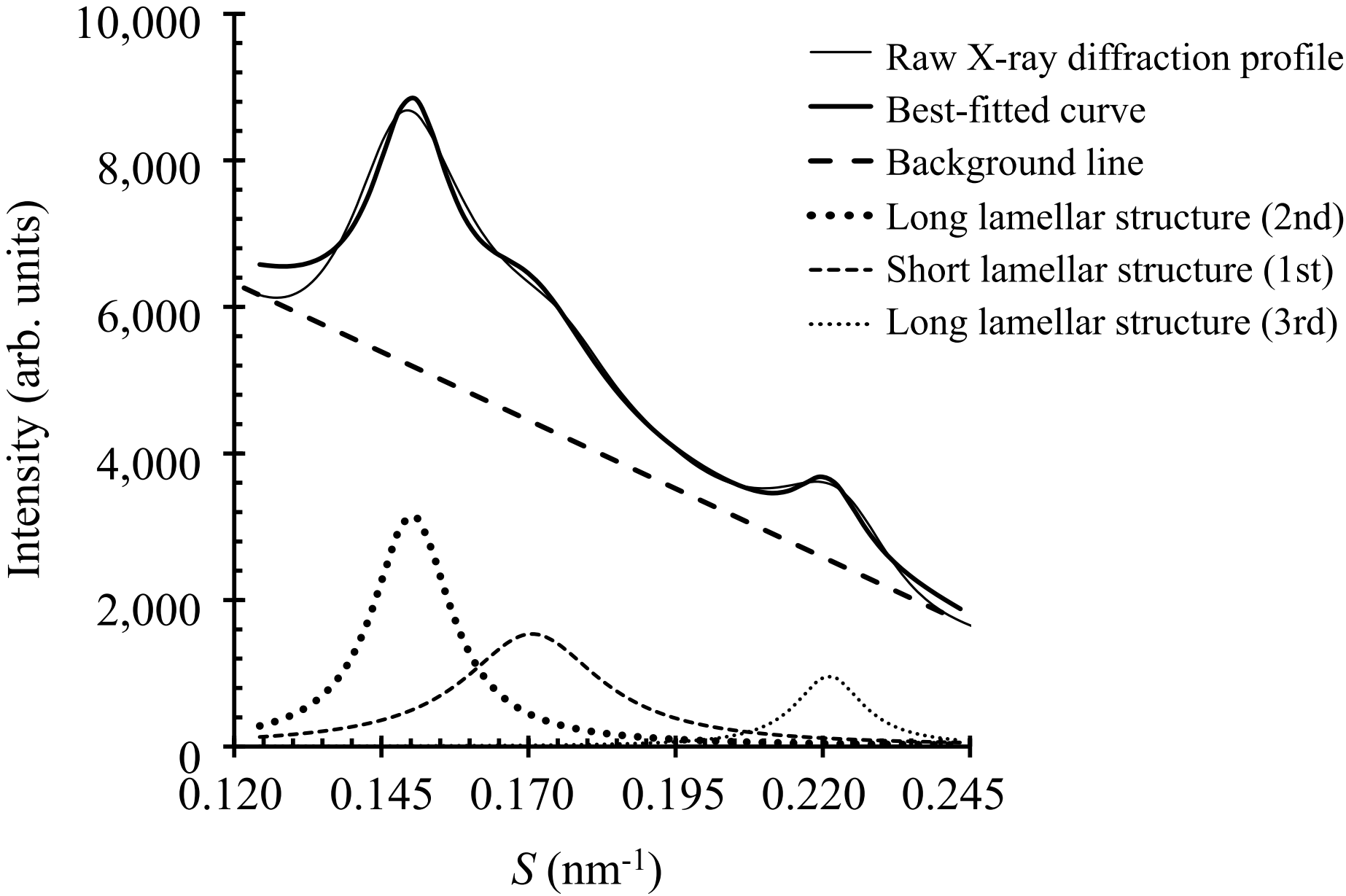
10,000
8,000
6,000
4,000
2,000
0
Intensity (arb. units)
0.120
0.145
0.170
0.195
0.220
0.245
S (nm-1)
Raw X-ray diffraction profile
Best-fitted curve
Background line
Long lamellar structure (2nd)
Short lamellar structure (1st)
Long lamellar structure (3rd)

**b** Fig. 3

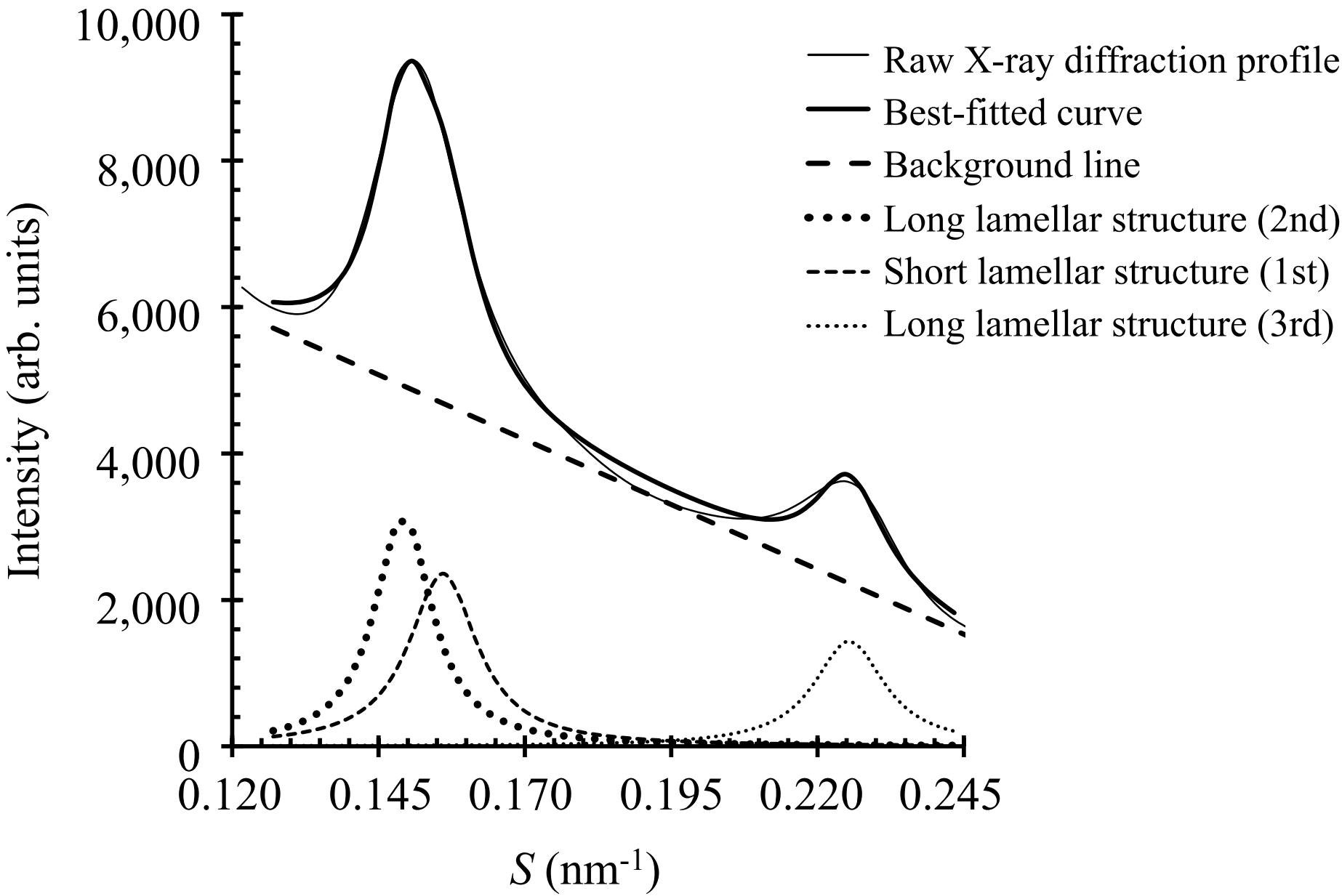
10,000
8,000
6,000
4,000
2,000
0
Intensity (arb. units)
0.120
0.145
0.170
0.195
0.220
0.245
S (nm-1)
Raw X-ray diffraction profile
Best-fitted curve
Background line
Long lamellar structure (2nd)
Short lamellar structure (1st)
Long lamellar structure (3rd)

**c** Fig. 3

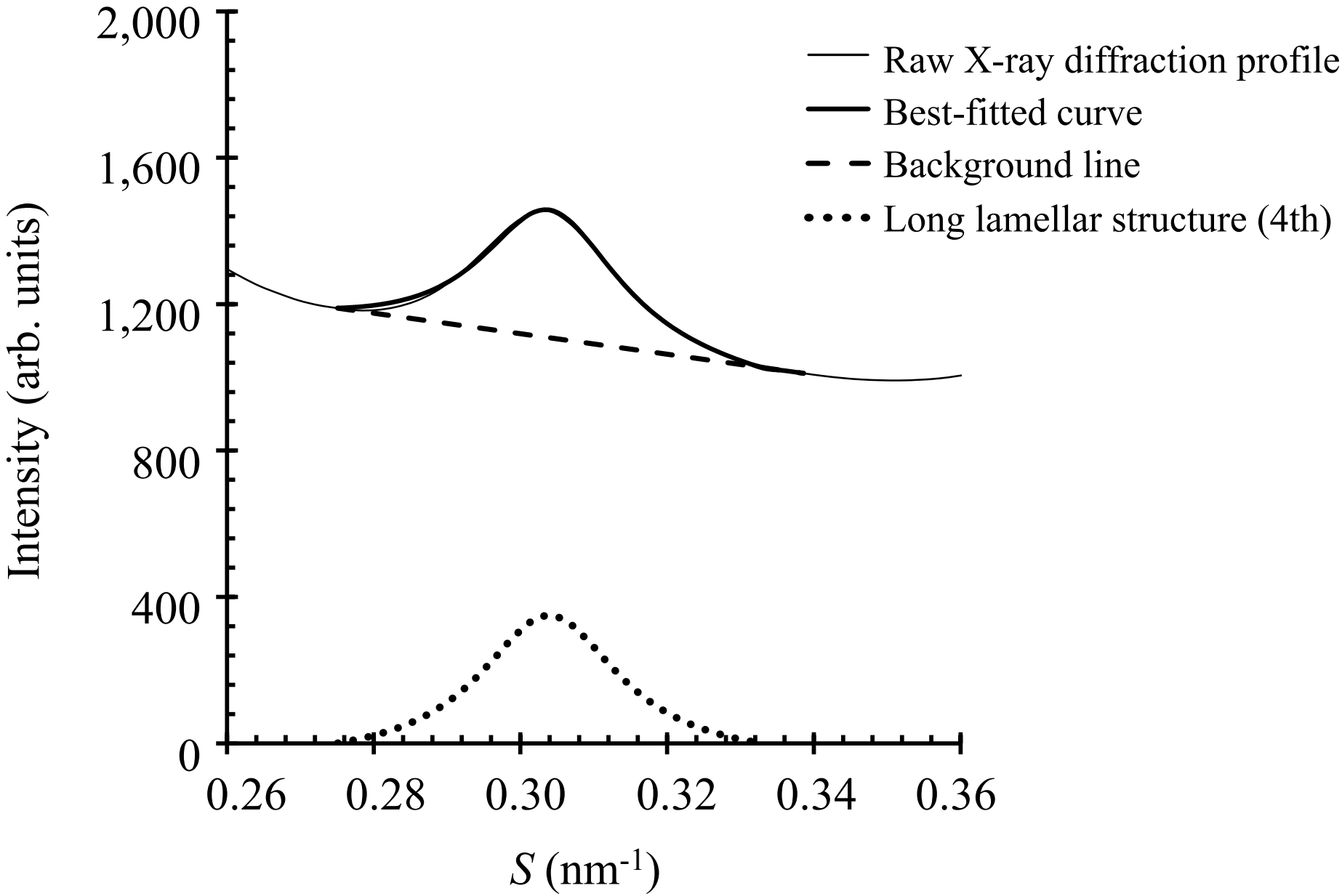
2,000
1,600
1,200
800
400
0
Intensity (arb. units)
0.26
0.28
0.30
0.32
0.34
0.36
S (nm-1)
Raw X-ray diffraction profile
Best-fitted curve
Background line
Long lamellar structure (4th)

Fig. 4

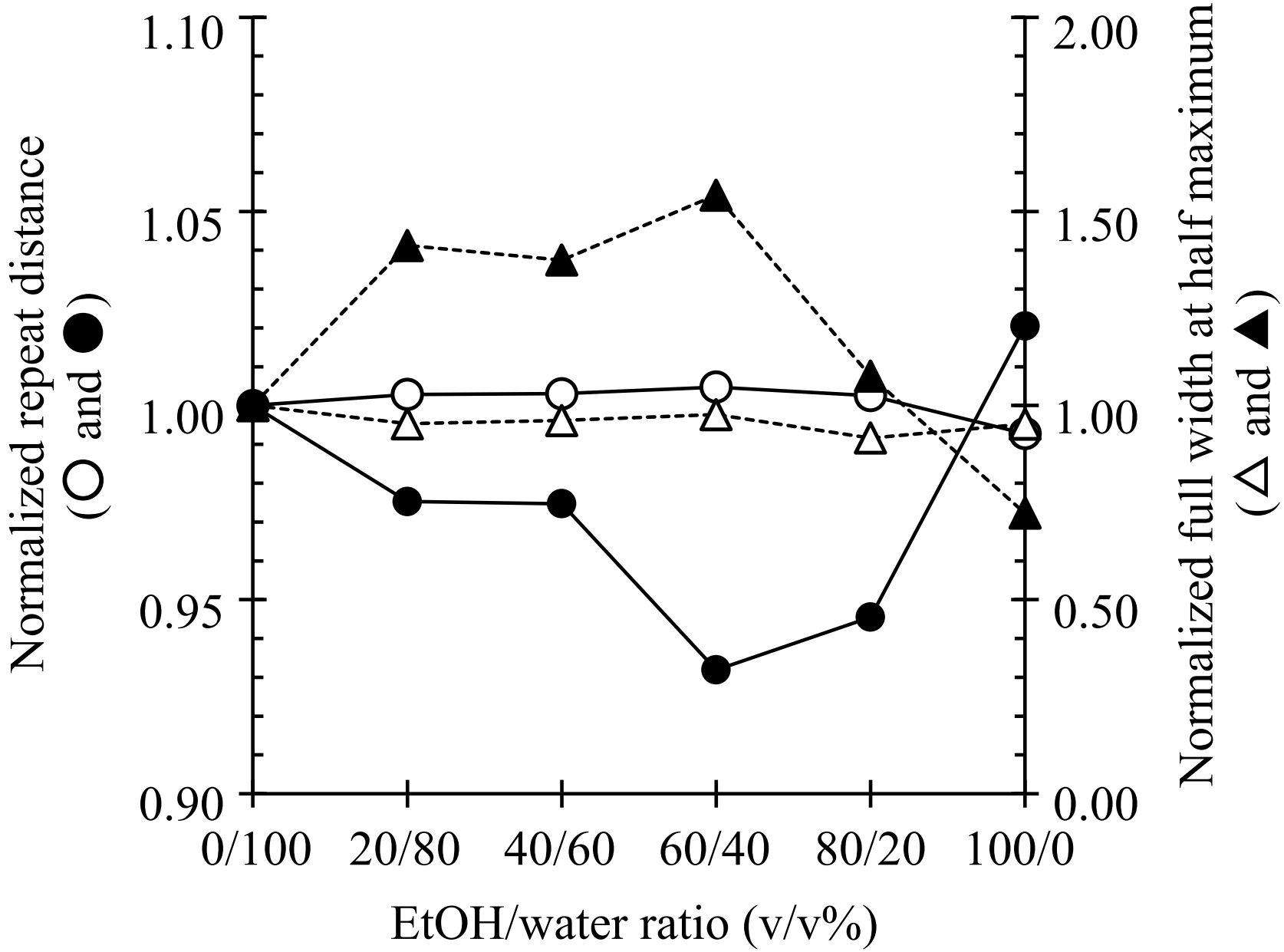
1.10
1.05
1.00
0.95
0.90
2.00
1.50
1.00
0.50
0.00
0/100
20/80
40/60
60/40
80/20
100/0
EtOH/water ratio (v/v%)
Normalized repeat distance
(O and ●)
Normalized full width at half maximum
(△ and ▲)

Fig. 5

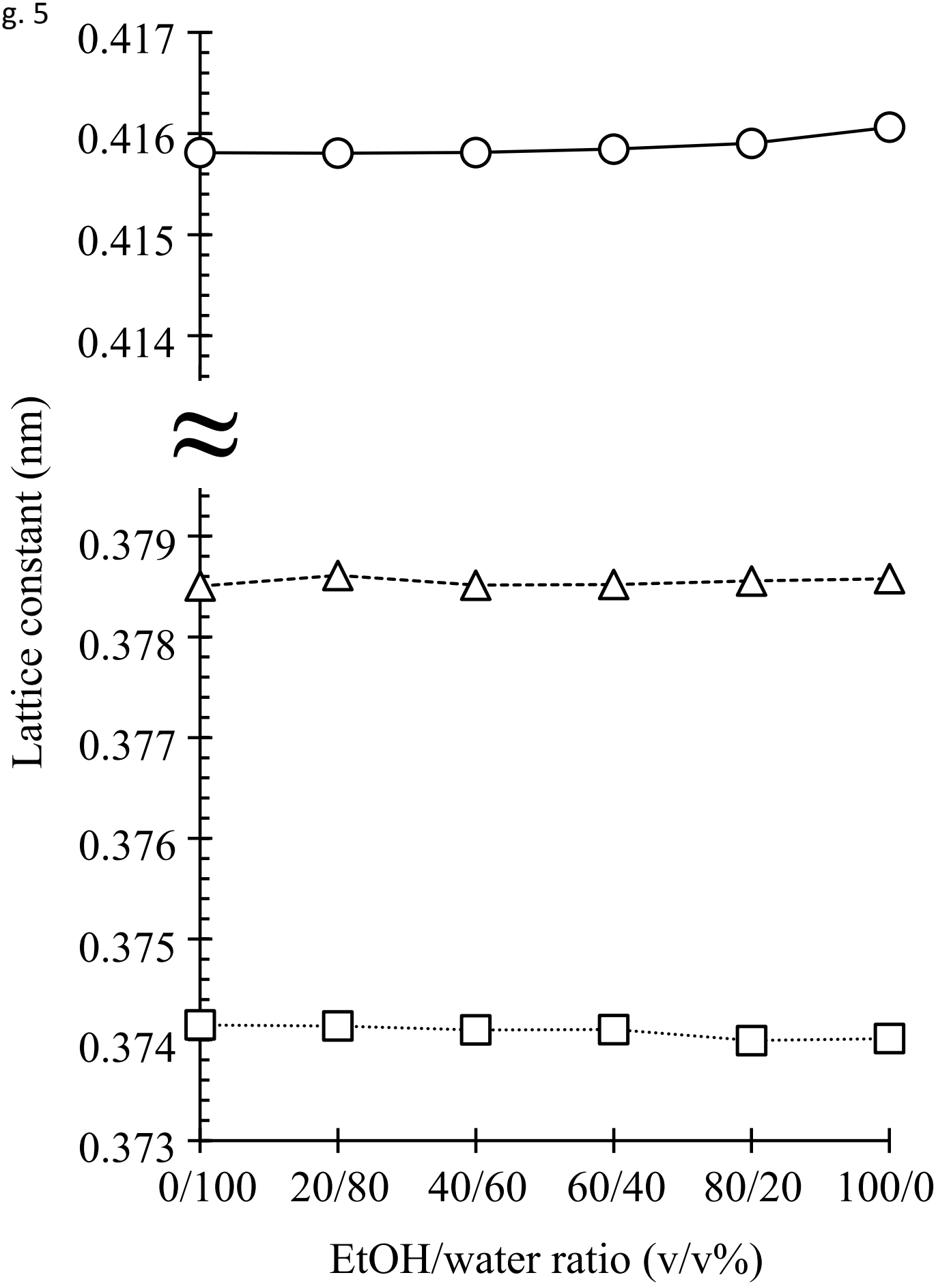
0.417
0.416
0.415
0.414
≈
0.379
0.378
0.377
0.376
0.375
0.374
0.373
Lattice constant (nm)
0/100
20/80
40/60
60/40
80/20
100/0
EtOH/water ratio (v/v%)

Fig. 6

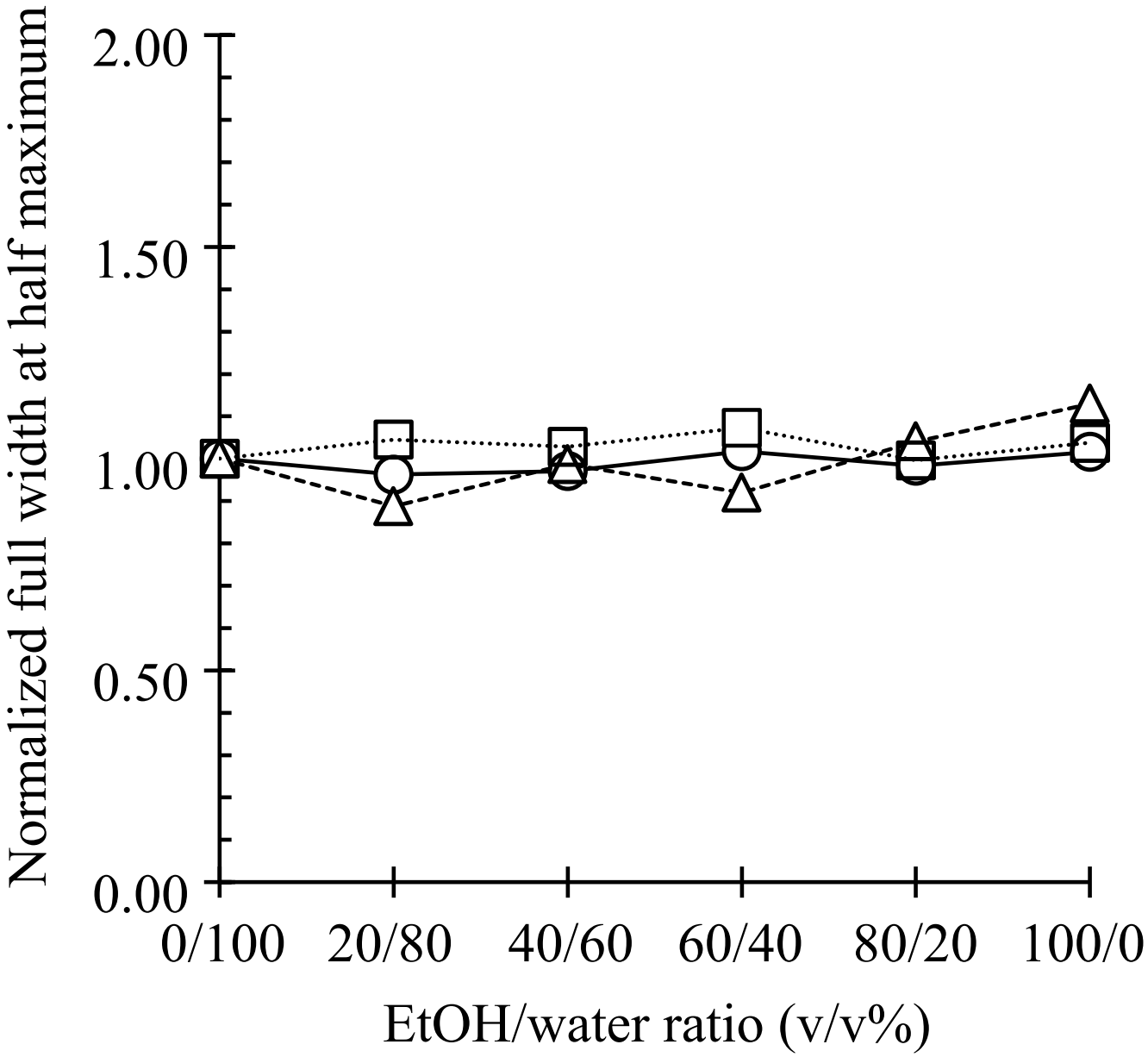
Normalized full width at half maximum
2.00
1.50
1.00
0.50
0.00
0/100
20/80
40/60
60/40
80/20
100/0
EtOH/water ratio (v/v%)

Fig. 7

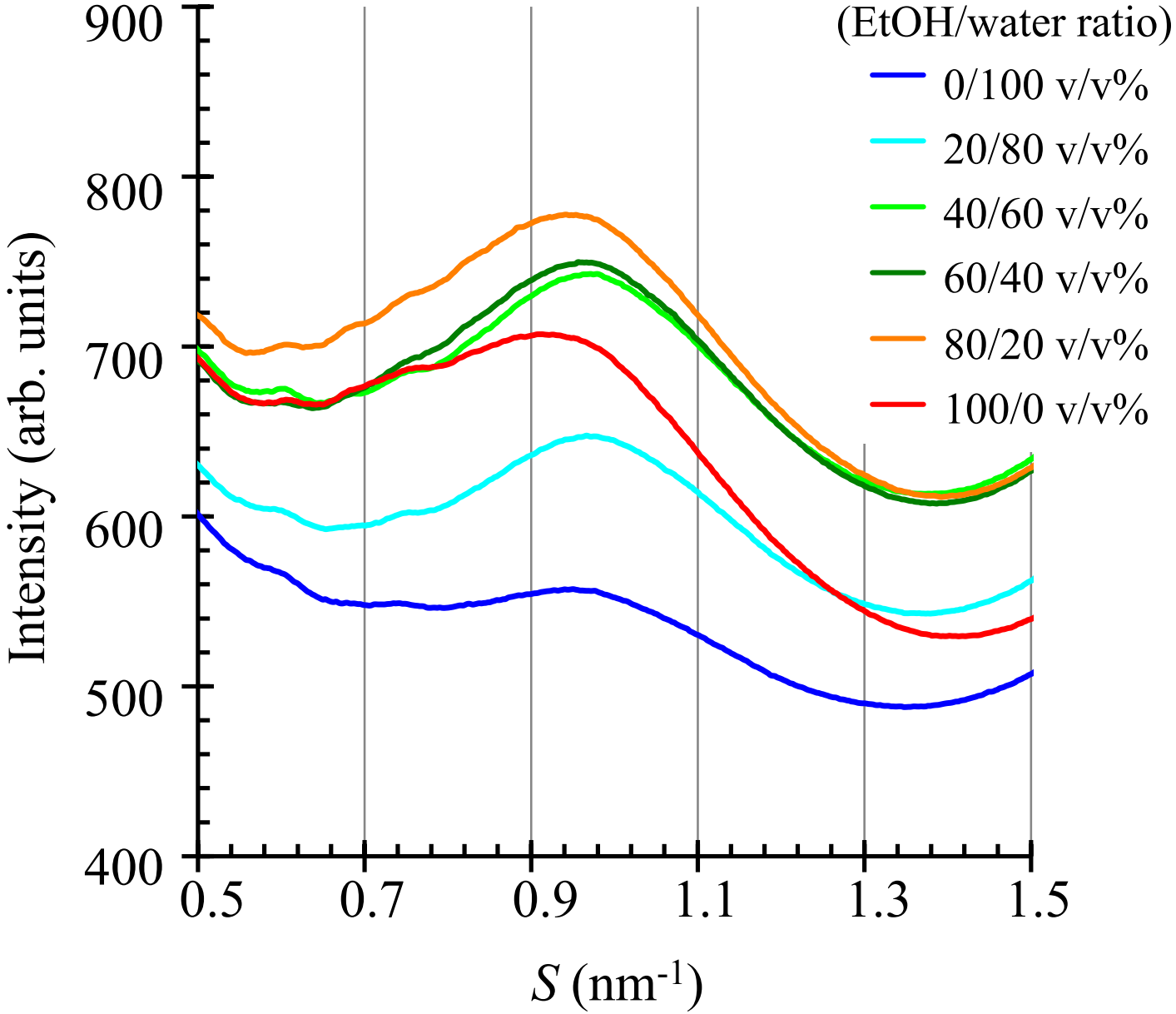
(EtOH/water ratio)
0/100 v/v%
20/80 v/v%
40/60 v/v%
60/40 v/v%
80/20 v/v%
100/0 v/v%
Intensity (arb. units)
900
800
700
600
500
400
0.5
0.7
0.9
1.1
1.3
1.5
S (nm-1)

Fig. 8

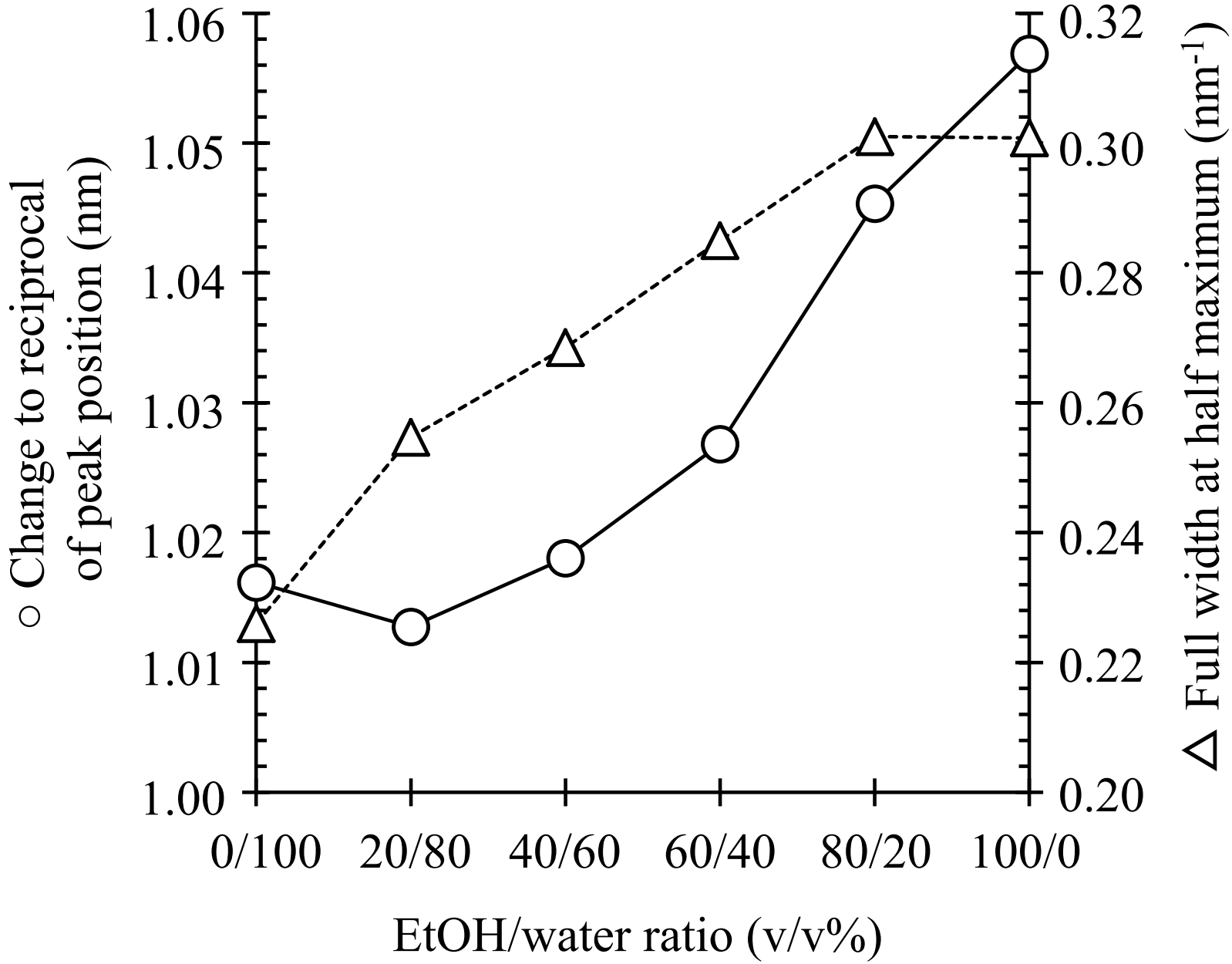
1.06
1.05
1.04
1.03
1.02
1.01
1.00
○ Change to reciprocal of peak position (nm)
0.32
0.30
0.28
0.26
0.24
0.22
0.20
△ Full width at half maximum (nm-1)
0/100
20/80
40/60
60/40
80/20
100/0
EtOH/water ratio (v/v%)